

Carbon nanotube electron windmills: a novel design for nano-motors.

S. W. D. Bailey, I. Amanatidis, and C. J. Lambert

Department of Physics, Lancaster University, Lancaster, LA1 4YB, U. K.

(Dated: October 26, 2018)

Abstract

We propose a new drive mechanism for carbon nanotube (CNT) motors, based upon the torque generated by a flux of electrons passing through a chiral nanotube. The structure of interest comprises a double-walled CNT, formed from, for example, an achiral outer tube encompassing a chiral inner tube. Through a detailed analysis of electrons passing through such a "windmill", we find that the current due to a potential difference applied to the outer CNT generates sufficient torque to overcome the static and dynamic frictional forces that exists between the inner and outer walls, thereby causing the inner tube to rotate.

PACS numbers: 73.63.-b,68.65.-k,71.15.Ap

arXiv:0806.1468v1 [cond-mat.mtrl-sci] 9 Jun 2008

The evolution from micro- to nano-electronics, as exemplified by the exponential growth in mobile communications and personal computing is paralleled by the more-recent miniaturisation of mechanical devices, which are currently undergoing a transition from commercially-available microelectromechanical structures (MEMS) to nanometre-scale nanoelectromechanical structures (NEMS). Whereas microfabricated motors, actuators and oscillators [1] are typically manufactured by conventional semiconductor processing techniques, their nanoscale counterparts are more difficult to realise.

An early example of an artificial NEMS [2], [3] is based on a telescoping structure formed from multiwalled carbon nanotubes (MWCNTs). These structures possess novel electrical properties [4] and extremely low inter-shell friction [5]. The latter discovery led to the idea of CNT nanomechanical oscillators [5], [6], [7], [8], [9] with gigahertz operation frequencies, which is beyond the reach of MEMS oscillators [10]. The ultra-low inter-shell friction in MWCNTs also underpins recently-developed CNT-based nanomotors [11], [12], which involve a MWCNT whose outer shell is clamped to two metallic anchor pads and whose inner shell (or shells) is free to rotate or oscillate. A metallic plate is deposited on the mobile shell and movement is induced via an electrostatic interaction between the metallic plate and external gates.

The aim of the present paper is to propose a new dc drive mechanism for CNT-based motors. For all such nano-mechanical devices analysed to date, the static forces can roughly be classified as elastic, electrostatic, friction and van der Waals. In this paper, we propose a new force, which has so far been ignored in the NEMS literature. This force provides a new "electron-turbine" drive mechanism for CNT-based nanomotors and obviates the need for metallic plates and gates in the nano-motor of [11], [12]. To understand the origin of this force, consider the structure shown in Fig. 1a, which comprises a double-walled CNT, formed from an achiral (18,0) outer tube clamped to external electrodes and a chiral (6,4) inner tube. As in [11], [12], the central region of the outer tube has been removed to expose the free-to-rotate, chiral inner tube. The proposed force arises when a dc voltage is applied between the external electrodes, which produces a "wind" of electrons (eg) from left to right. The incident electron flux (from the achiral CNT) possesses zero angular momentum, whereas after interacting with the chiral nanotube, the outgoing current carries a finite angular momentum. By Newton's third law, this flux of angular momentum produces a tangential force (and an associated torque) on the inner nanotube, causing it to rotate.

Fig. 1b shows an even simpler version of this motor, which we refer to as a CNT "drill", which comprises an achiral outer tube clamped to an external electrode and a free-to-rotate, chiral inner

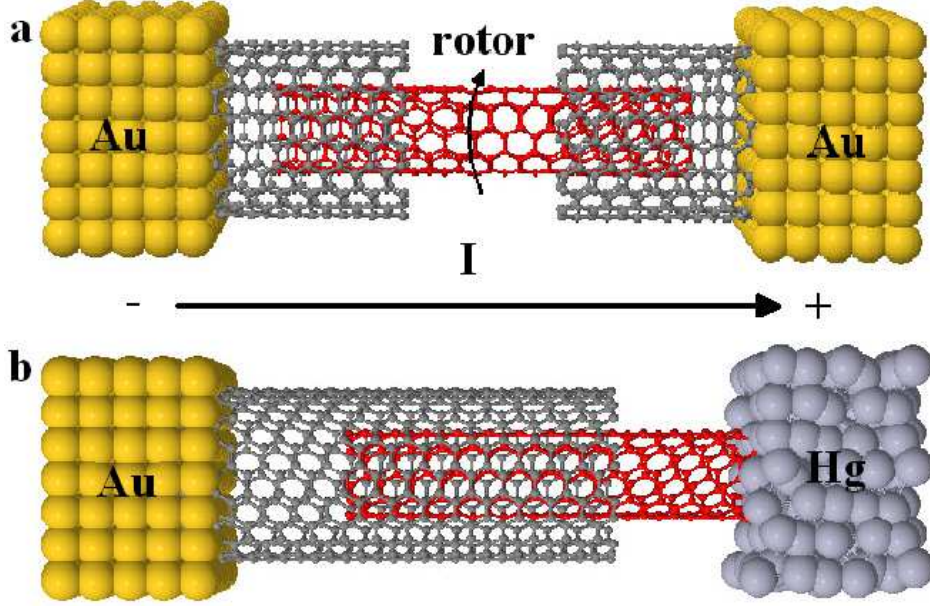


FIG. 1: The proposed nano-motor (1a) and nano-drill (1b) formed from an inner (6,4) CNT (red) and an outer (18,0) CNT (grey). The nano-motor is attached to gold electrodes, which act as reservoirs of electrons, whereas the nano-drill has one end contacted to a mercury electrode.

tube contacted to a mercury bath, as in [13].

The main question, is whether or not this new force is sufficient to overcome frictional forces between the inner and outer tube. The central result of our calculations, is that for moderate voltages, the tangential force produced by the electron wind can significantly exceed the frictional forces and therefore electron windmills provide a viable alternative to electrostatic nano-motors realised to date. This result is illustrated in Fig. 2a, which shows the tangential force (F_{motor}) as a function of the applied voltage (ϕ), exerted on the (18,0)@(6,4) drill of Fig. 1b. In this example, the number of overlap atoms (N_{atoms}) between the inner (6,4) and the outer (18,0) CNT is approximately 4000 and since the static friction is $F_{\text{exp}} \approx 10^{-15}$ N/atom [14], the total static friction is $F_c \approx 4.10^{-12}$. Fig. 2a shows that when ϕ is approximately 0.4 volts, F_{motor} exceeds F_c by almost three orders of magnitude.

Before describing the theory leading to Fig. 2, it is also of interest to ask if F_{motor} can overcome the dynamical friction between the two CNTs [15], [16], [17]. For a spinning CNT with carbon atoms of mass m_c moving with a tangential velocity v_c , the dynamical friction force per carbon atom is [17] $m_c v_c / \tau$, where $\tau \approx 0.5 \text{ ns}$. Equating the dynamical friction to F_{motor} yields a maximum tangential velocity of $v_{\text{max}} \approx 10^7 \alpha / N_c \text{ ms}^{-1}$, where N_c is the number of overlap atoms and

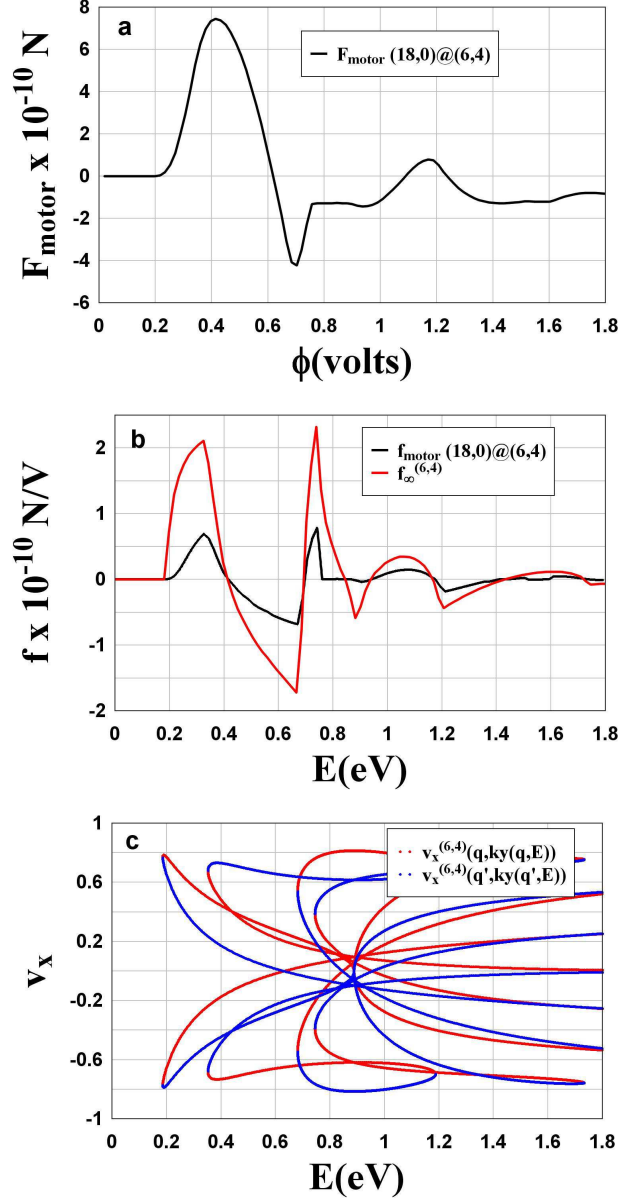


FIG. 2: (a) The tangential force (F_{motor}) exerted on a $(18,0)@(6,4)$ nano-drill as a function of the voltage ϕ . (b). The black curve shows the computed tangential force per volt $f_{\text{motor}}(E)$ for the $(18,0)@(6,4)$ drill, whose integral yields the curve in fig 1a, in accordance with Equ. (7). For comparison, the red curve shows the quantity $f_{\infty}^{(6,4)}(E)$ of equation (12), which is proportional to the total tangential velocity carried by all right-moving channels of energy E in an infinite $(6,4)$ chiral CNT. (c) A "fan diagram" showing the tangential velocities (c) $v_x^{(6,4)}(q, k_y(q, E))/v_F$ carried by right-moving channels q (red) and left-moving channels q' (blue) of an infinite $(6,4)$ chiral CNT. The red curves sum to yield the red curve of fig 2b, in accordance with Equ. (10).

$\alpha = F_{\text{motor}}/F_0$, where $F_0 = 4.1 \cdot 10^{-10} N$ is a natural unit of force (see below). This means that even for moderate voltages, the electron wind is sufficient to drive the inner tube to the mechanical breakdown velocity ($\approx 8 \cdot 10^3 m s^{-1}$) [17].

This demonstration that an "electron wind" can cause a chiral "CNT windmill" to rotate, could lead to range of applications [18]. By analogy with the occurrence of spin torques in magnetic point contacts and tunnel junctions[19],[20], which have applications in nanoscale magnetic memory devices, one expects CNT windmills to have nanoscale memory applications. For example, a voltage pulse through a CNT motor would cause the inner element to rotate by a pre-determined angle, which may be utilized in a switch or memory element. A rotating chiral CNT in contact with a reservoir of atoms or molecules could act as a nano-fluidic pump.

We now present details of the calculations leading to Fig 2a. To calculate the rotational driving force, we note that the momentum of an electron wavepacket incident along a semi-infinite CNT is equal to the mass of the electron multiplied by its group velocity. To quantify the tangential momentum, consider an (n, m) CNT defined by a chiral vector $\mathbf{C}_h = n\mathbf{a}_1 + m\mathbf{a}_2$ and a translation vector $\mathbf{T}_r = t_1\mathbf{a}_1 + t_2\mathbf{a}_2$, where $(0 \leq m \leq n)$, $\mathbf{a}_1, \mathbf{a}_2$ are the lattice vectors, $t_1 = (2m + n)/d_r$ and $t_2 = -(2n + m)/d_r$ with d_r the greatest common divisor of $(2n + m, 2m + n)$.

For electrons with group velocity \mathbf{v} , we define the longitudinal component of the velocity to be $v_y = \mathbf{v} \cdot \mathbf{T}_r$ and the transverse to be $v_x = \mathbf{v} \cdot \mathbf{C}_h$. The quantized component k_x of the wave vector $\mathbf{k} = (k_x, k_y)$ parallel to the chiral vector satisfies

$$k_x^q = \frac{2\pi q}{L}, (q = 1, \dots, N_{hex}),$$

where $N_{hex} = 2L^2/(a^2 d_r)$ is the number of hexagons in the CNT unit cell with L the length of the chiral vector and a the length of the lattice vector. For a given value of the quantized wavevector k_x^q , the energy of an electron is a function $E(k_x^q, k_y)$ of the continuous, longitudinal component k_y of the wavevector, which satisfies

$$-\frac{\pi}{|\mathbf{T}_r|} < k_y a < +\frac{\pi}{|\mathbf{T}_r|}.$$

For example, within a minimal tight-binding model of π bonding in graphene, with a parameterized tight binding transfer integral γ , the 1-D dispersion curves for such a CNT, are given

by

$$\begin{aligned}
E(k_x, k_y) = & \pm\gamma\left(1 + 4\cos\frac{\sqrt{3}}{2}(k_x a \cos\theta - k_y a \sin\theta)\right. \\
& \left.\cos\frac{1}{2}(k_x a \sin\theta + k_y a \cos\theta) + \right. \\
& \left. 4\cos^2\frac{1}{2}(k_x a \sin\theta + k_y a \cos\theta)\right)^{1/2}
\end{aligned} \tag{1}$$

where $\tan\theta = (n - m)/\sqrt{3}(n + m)$ (i.e. θ is $\pi/6$ minus the chiral angle). For all electrons of energy E moving along a 1-d channel of quantum number q , the equation $E(k_x^q, k_y) = E$ can be solved to yield two E -dependent values of k_y , which we denote by $k_y(q, E)$ and $-k_y(q', E)$, corresponding to positive (ie. right-moving) and negative (ie. left-moving) longitudinal group velocities $v_y(q, k_y)$ and $v_y(q', -k_y)$ respectively, where $v_y(q, k_y) = (1/\hbar)\partial E(k_x^q, k_y)/\partial k_y$. The corresponding tangential group velocities are $v_x(q, k_y)$ and $v_x(q', -k_y)$ respectively, where $v_x(q, k_y) = (1/\hbar)\partial E(k_x^q, k_y)/\partial k_x^q$.

For an $(n', m')@ (n, m)$ structure of the kind shown in Fig. 1, which is derived from a chiral (n, m) CNT inside an achiral (n', m') CNT, a right moving electron of energy E incident along channel q , with tangential group velocity $v_x(q, k_y(q, E))$ will either be reflected into left-moving channels q' of the left CNT with tangential group velocities $v_x(q', -k_y(q', E))$ and reflection probability $R_{q'q}(E)$ or it will be transmitted into right-moving channels q' of the right CNT with tangential group velocities $v_x(q', k_y(q', E))$ and transmission probability $T_{q'q}(E)$.

The flux of tangential momentum into the motor is

$$\begin{aligned}
P_{\text{motor}} = & \frac{2m_e}{h} \\
& \int_{-\infty}^{\infty} dE [v_{\text{in}}(E) - v_{\text{out}}(E)] [f_{\text{left}}(E) - f_{\text{right}}(E)]
\end{aligned} \tag{2}$$

where $f_{\text{left}}(E)$ and $f_{\text{right}}(E)$ are Fermi distributions for incoming channels from the left and right reservoirs and

$$v_{\text{in}} = \sum_q v_x(q, k_y(q, E)). \tag{3}$$

Furthermore,

$$v_{\text{out}}(E) = v_{\text{R}}(E) + v_{\text{T}}(E), \tag{4}$$

where

$$v_{\text{R}}(E) = \sum_{q'q} [v_x(q', -k_y(q', E))R_{q'q}(E)] \tag{5}$$

$$v_T(E) = \sum_{q'q} [v_x(q', k_y(q', E)) T_{q'q}(E)] \quad (6)$$

In these equations, q sums over incoming channels and q' sums over outgoing channels. Eq. (2) is valid even if both CNTs are chiral. By symmetry, for the case considered here, where the outer CNT is achiral, $v_{in}(E) = 0$. It can also be demonstrated that for the case of total reflection, where $T_{q'q}(E) = 0$ (for all q', q), equation (4) yields $v_{out}(E) = 0$.

By Newton's third law, the net tangential force exerted on the inner chiral CNT is $F_{motor} = -P_{motor}$ and therefore

$$F_{motor} = \int_{-\infty}^{\infty} \frac{dE}{e} f_{motor}(E) [f_{left}(E) - f_{right}(E)] \quad (7)$$

where $f_{motor}(E)$ is the tangential force per volt due to electrons of energy E , given by

$$f_{motor}(E) = f_0 [v_{out}(E) - v_{in}(E)] / v_F, \quad (8)$$

with f_0 the characteristic tangential force per volt, given by

$$f_0 = \frac{2m_e e}{h} v_F. \quad (9)$$

For metallic CNTs, $v_F = 9.35 \times 10^5$ m/s and therefore $f_0 = 4.12 \times 10^{-10}$ N/V. (The corresponding force at 1 volt is $F_0 = 4.12 \times 10^{-10}$ N and is the natural unit of force introduced above.) We note that if $e\phi$ is the chemical potential difference between the reservoirs and if $e\phi$ is small compared with $k_B T$, then $[f_{left}(E) - f_{right}(E)] \approx e\phi [-\partial f(E) / \partial E]$, which reduces to $e\phi \delta(E - E_F)$ in the limit $k_B T \rightarrow 0$. On the other hand if $k_B T$ is small compared with $e\phi$, then $[f_{left}(E) - f_{right}(E)]$ is of order unity within an energy interval of order $e\phi$ and zero outside this interval. In what follows, for the purpose of proving the viability of the proposed motor, we shall focus on the latter regime.

For a $(n', m') @ (n, m)$ motor with an achiral (n', m') outer CNT, an upper bound for the tangential force is obtained by setting $v_{in} = 0$ and replacing v_{out} by the maximum possible tangential velocity carried by right-moving channels of an infinite (n, m) chiral CNT. In units of v_F this is given by

$$v_{\infty}^{(n,m)}(E) = \sum_q v_x^{(n,m)}(q, k_y(q, E)) / v_F, \quad (10)$$

where $v_x^{(n,m)}(q, k_y(q, E)) / v_F$ is the dimensionless tangential group velocity of a right moving channel q of an infinite (n, m) CNT.

The flux of tangential momentum carried by these electrons yields an upper bound on the tangential force of the corresponding motor, given by

$$F_{\infty}^{(n,m)}(e\phi) = \int_{-e\phi/2}^{e\phi/2} \frac{dE}{e} f_{\infty}^{(n,m)}(E), \quad (11)$$

where $f_{\infty}^{(n,m)}(E)$ is the flux of tangential momentum per volt due to electrons of energy E , given by

$$f_{\infty}^{(n,m)}(E) = f_0 v_{\infty}^{(n,m)}(E). \quad (12)$$

The latter quantity is shown as the red curve in Fig. 2b, whereas the black curve shows the tangential force per volt, obtained by computing all scattering coefficients and evaluating equation (8).

To understand the origin of the oscillations in $f_{\infty}^{(n,m)}(E)$, the red curves in Fig. 2c show the values of $v_x^{(6,4)}(q, k_y(q, E))/v_F$ for right-moving channels. (for comparison, the blue curves show $v_x^{(6,4)}(q', k_y(q', E))/v_F$ for left-moving channels). In equation (10), the label q sums over $N(E)$ open channels of the CNT, where $N(E)$ is an integer given by $N(E) = \sum_q$. Clearly $N(E)$ is a discontinuous function of E , which changes by an integer whenever new channels open or close. As shown by the red curves in Fig. 2c, right-moving channels open or close in pairs and just as a pair of channels open, their tangential velocities cancel. Consequently, $v_{\infty}^{(6,4)}(E)$ is a continuous function of E , with a discontinuous first derivative.

The red curve of Fig. 2b shows that the tangential velocity of right-moving electrons in an infinite chiral CNT is an oscillatory function of E , whose slope changes whenever new channels open. The black curve of Fig. 2b shows that these oscillations are also present in $f_{\text{motor}}(E)$. To compute $f_{\text{motor}}(E)$, we used a parameterized single-state π orbital Hamiltonian, based on a global fit to density functional results for graphite, diamond and C_2 as a function of the lattice parameter [21]. This gives good agreement with the single π orbital interaction between two carbon atoms separated by $d = 3.40\text{\AA}$ predicted by [23] of 0.35 eV and is appropriate to our system, where the inter-wall separation is $d = 3.65\text{\AA}$. A recursive Greens function formalism was then used to evaluate the transmission matrix \mathbf{t} , describing the scattering of electrons of energy E from one end of the semi-infinite nanotube to the other [22].

The tangential force shown in Fig. 2a is obtained by integrating the black curve of Fig. 2b over the applied voltage, in accordance with equation (7). The result depends slightly on the orientation of the inner tube relative to the outer tube and therefore the results shown in Fig. 2a is averaged over

all orientations. We have carried out calculations which demonstrate the viabilities of CNT motors and drills with a wide variety of chiralities and inter-tube couplings. The result is rather robust and does not depend strongly on the number of overlap atoms, provided the electrons evolving from the outer to the inner tube do not strongly back scatter. If the intertube coupling causes strong back scattering, then the tangential force is reduced, but oscillations of the form shown in Fig. 2b persist. Fig. 2b demonstrates that the tangential force vanishes for energies below approx. 0.19 eV, since there are no open channels in the chiral (6,4) CNT. It is interesting to note that a voltage threshold also occurs when the achiral outer CNT is chosen to be an armchair tube, because the two channels closest to the Fermi energy possess vanishing tangential velocities and therefore electrons in these channels cannot exert a tangential force. In all cases, the voltage threshold can be removed by tuning the Fermi energy to coincide with open channels of the outer CNT carrying a finite tangential velocity.

In summary, we have highlighted a new force, arising from an electron wind impinging on a chiral CNT, which is capable of overcoming measured friction forces and driving a rotational CNT motor or drill. This may open a new route to low-power, non-volatile nanoscale memory and could have applications to nanofluidics. For the future, it will be of interest to examine other drive mechanisms for chiral CNT motors. For example, if the electrical contacts in Fig. 1 are replaced by reservoirs of atoms or molecules and a pressure difference applied to drive the atoms or molecules from left to right, then the resulting transfer of angular momentum may also be sufficient to drive the motor, as could a flux of phonons resulting from a temperature difference between the ends of the device.

Finally, we note that other mechanisms for driving CNT motors have been proposed, based on ac fields. In the case of [24] this involves the use of circularly polarized light, whereas [25] involves a brownian ratchet. The force produced by the former is 2-3 orders of magnitude smaller than the drive mechanism discussed in the present paper, while the latter requires a high-frequency drive voltage. By dispensing with the need for electrostatic gates and ac voltages, fewer processing steps are needed to construct the electron turbines of Fig 1.

Acknowledgements.

This work is supported by the EPSRC, the EU MCRTN Fundamentals of Nanoelectronics, the DTI, the RCUK Basic Technology programme and North West Science Grid .

-
- [1] W. Trimmer, *Micromechanics and MEMS: Classic and seminal papers to 1990* (IEEE Press, New York 1997)
- [2] J. Cummings and A. Zettl, *Science* **289**, 602 (2000)
- [3] M-F Yu, B.I. Yakobson and R.S. Ruoff, *J. Chem. B* **104**, 8764 (2000)
- [4] I. M. Grace, S. W. Bailey and C. J. Lambert, *Phys. Rev. B* **70**, 153405 (2004)
- [5] A. N. Kolmogorov and V. H. Crespi, *Phys. Rev. Lett.* **85**, 4727, (2000).
- [6] S. B. Legoas et al *Phys. Rev. Lett.* **88**, 045503 (2002).
- [7] Q. Zheng and Q. Jiang, *Phys. Rev. Lett.* **88**, 045503 (2002)
- [8] L. Forro, *Science* **289** 560 (2000)
- [9] P.A. Williams et al *Phys. Rev. Lett.* **89** 255502 (2002)
- [10] J. L. Rivera, C. McCabe and P. T. Cummings, *Nano Letters*, **3**, 1001 (2003)
- [11] A.M. Fennimore et al, *Nature* **424** 408 (2003)
- [12] B. Bourlon, D.C. Glattli, C. Miko, L. Forro and A. Bachtold, *Nano Lett.* **4**, 709 (2004).
- [13] S. Franck et al, *Science* **280** (1998).
- [14] A. Kis, K. Jensen, S. Aloni, W. Mickelson and A. Zettl. *Phys. Rev. Lett.* **97**, 025501 (2006).
- [15] S. Zhang, W. K. Liu and R. S. Ruoff, *Nano Lett.* **4**, 293 (2004)
- [16] J. Servante and P. Gaspard, *Phys. Rev. B.* **73**, 125428 (2006).
- [17] J. Servante and P. Gaspard, *Phys. Rev. Lett.* **97**, 186106 (2006).
- [18] C.J. Lambert, The Patents Office, Patents Directorate, no. GB2422638, August (2006)
- [19] S. I. Kiselev et al., *Nature (London)* **425**, **380** (2003).
- [20] G. D. Fuchs et al, *Phys. Rev. Lett.* **96**, 186603 (2006)
- [21] D. Tománek and M. A. Schluter, *Phys. Rev. Lett.* **67**, 2331 (1991).
- [22] S. Sanvito, C. J. Lambert and J. H. Jefferson, *Phys. Rev. B.* **59**, 11936 (1999).
- [23] R. Saito, G. Dresselhaus, M. S. Dresselhaus, *Physical Properties of Carbon Nanotubes*. Imperial College London, 1998.
- [24] P. Kral and H. R. Sadeghpour, *Phys. Rev. B.* **65**, 161401, (2002).
- [25] Z. C. Tu and X. Hu. *Phys. Rev. B* **72** 033404 (2005).